Journal of Engineering and Science Research 7 (3): 32-37, 2023
e-ISSN: 2289-7127

DOI: 10.26666/rmp.jesr.2023.3.5

Magnetic Characteristics of a Magnetorheological Elastomer Bushing

Mahmud Iskandar Seth A Rahim[1,*], Nasrul Shukri Nasir[1], Shamsul Kamaruddin[2], Nazirah Ahmad[1]

[1]Technology & Engineering Division, RRIM Research Station, Lembaga Getah Malaysia, 47000, Sungai Buloh, Selangor, Malaysia.
[2]Quality & Technical Service Division, RRIM Research Station, Lembaga Getah Malaysia, 47000, Sungai Buloh, Selangor, Malaysia.

*Corresponding Author: mahmud@lgm.gov.my

Received: 01 April 2023; Revised: 15 April 2023; Accepted: 15 May 2023; Published: 30 June 2023

Abstract: The present study aims to investigate the magnetic characteristics of a magnetorheological elastomer (MRE) bushing for design optimization in the high-frequency dynamic test. The proposed design consists of MRE bushing covered cylindrically with the coil bobbin for electromagnetic coil winding. These components are covered with the testing jig attached to the testing machine. MRE experimental studies often show uncertainty in evaluating the magnetic distribution across the entire testing structure specifically in MRE specimens. A finite element model for MRE bushing is designed to evaluate the magnetic distribution of the device under several factors that can affect the magnetic distribution. The results of the model are optimized to obtain high magnetic flux density in the MRE area. The magnetic intensity (H) as a function of magnetic flux density (B) was also determined through the B-H relation curve. It was proved that the magnetic distribution is affected significantly by factors such as material components and current applied (Ampere) to the MRE bushing. The optimum MRE bushing design with 1 Ampere can reach the highest magnetic flux density of 960 mT. Therefore, an optimum magnetic distribution condition for MRE bushing can be realized in the real experimental study.

Keywords: *Magnetorheological Elastomer, MRE Bushing, Automotive, Finite Element, Magnetic Flux Density.*

1. Introduction

Magnetorheological elastomers (MRE) are classified as one of the smart materials. This material consists of magnetizable particles in the non-magnetic elastomer matrix. In the presence of an external magnetic field, the material can switch its magnetic field-dependent properties, resulting in its ability to control stiffness and damping behavior. This characteristic makes MRE a promising candidate over the existing materials for various automotive applications such as vibration absorbers [1] and vibration isolators [2].

Recently, several MRE researchers have started a new approach to predict the magnetic distribution in real engineering testing using a finite element model. Finite Element Method Magnetics (FEMM) software is a set of programs for solving low-frequency electromagnetic problems on two-dimensional planar and axisymmetric domains. The usage of this software is becoming an attraction among MRE researchers as it can predict the direction of the magnetic field during MRE testing. This virtual analysis can help design the magnetic circuit in the actual MRE testing by simulating the magnetic field in different conditions and parameters. Table 1 summarizes the application of FEMM software in MRE research.

Corresponding Author: Mahmud Iskandar Seth A Rahim, Technology & Engineering Division, RRIM Research Station, Lembaga Getah Malaysia, 47000, Sungai Buloh, Selangor, Malaysia. Email: mahmud@lgm.gov.my

Table 1
Review summary on FEMM application in MRE research.

MRE Matrix	Magnet Types	FEMM Conditions	Max Magnetic Flux Density	Author
Natural rubber	Electro magnet	2700 coil turns, at 0.5 to 1.4 Amp	85 mT	Agirre-Olabide et al., 2018 [3]
Ground tire rubber	Electro magnet	491 coil turns of 22 SWG copper wire, at 0 to 1.05 Amp	320 mT	Ubaidillah et al., 2018 [4]
Natural rubber	Permanent magnet, N35	-	900 mT	Woo Lee et al., 2018 [5]
Silicone rubber	Electro magnet	1000 coil turns of 18 AWG copper wire, at 0.5 to 2 Amp	170 mT	Priyandoko et al., 2019 [6]
Silicone rubber	Pemanent magnet, N52	-	390 mT	Khayam et al., 2020 [7]
Silicone rubber	Electro magnet	2.5 to 5 Amp	804 mT	Khanouki et al., 2020 [8]
Silicone rubber	Electro magnet and Permanent magnet, N45	2000 coil turns of 18 AWG copper wire,	200 mT	Fakhree et al., 2021 [9]
Natural rubber	Electro magnet	3500 coil turns of 24 SWG copper wire, at 0.4 to 2.4 Amp	310 mT	Mat Song et al., 2022 [10]
Natural rubber	Electro magnet	3500 coil turns of 24 SWG copper wire, at 0.5 to 2.5 Amp	205 mT	Abdul Hamid et al., 2023 [11]

The main elements of MREs are the matrix material which is a non-magnetic polymer matrix. As for the FEMM comparison study, most of the researchers focus on the two main rubber matrixes, natural rubber and silicone rubber. The selection of matrix material highly influences the dynamic modulus and MR effect of MREs [12]. In this case, the researcher must know the end application of their developed MRE to achieve an optimal balance between the dynamic modulus and MR effect. In the case of magnet types, there are two approaches that have been implemented. The first approach was an electromagnet with a coil and the second approach was a permanent magnet. Both approaches can be used to apply the magnetic field to the MRE sample during testing. The important information from this review is to see the typical conditions used in the FEMM software. Three main conditions affecting magnetic distribution are the number of coils turns, the diameter of the coil (American Wire Gauge: AWG or Standard Wire Gauge: SWG), and the current applied (Ampere). Each study investigated different FEMM conditions. The highest number of coil turns applied was 3500 turns [10,11] and the common current applied was below 5 Amp.

In the present study, the magnetic distribution of MRE bushing using FEMM software was investigated. The analysis was performed by studying several factors that can affect magnetic distribution and understand its behaviour to these factors. Finally, the magnetic characteristic input was applied to this analysis so that the software is able to show the real magnetic distribution behaviour for MRE bushing testing.

2. Experimental

The concept for MRE testing was designed to ensure the simplicity and practicability of the testing. Figure 1 shows the schematic of testing assembly parts during MRE bushing testing with the application of an electromagnetic coil. The testing design was first adapted from Mat Song *et al.* [10] and Abdul Hamid *et al.* [11]. These designs were then improvised and simplified by removing top and bottom plates covering the whole MRE bushing testing assembly.

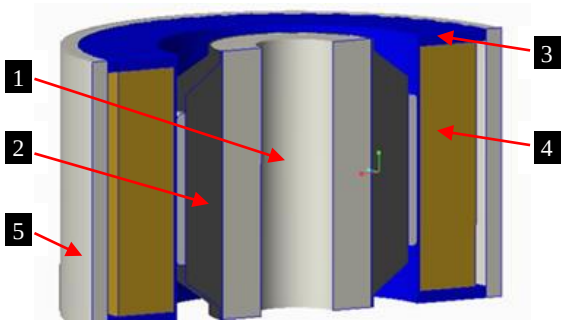

Figure 1. Cross-sectional drawing of the MRE testing design; (1) MRE bushing; (2) MRE; (3) coil bobbin; (4) electromagnet coil winding; and (5) housing.

The first part is MRE bushing (1). The internal core and the external casing are separated by the MRE sample (2). This bushing will be inserted inside the coil bobbin (3), and an electromagnetic coil (4) winding around the bobbin. The current (Ampere) will be supplied and directed along the electromagnetic coil and the magnetic flux will be generated and circulated toward the MRE area. Finally, the coil bobbin consisting of the MRE bushing will be inserted inside the testing jig or housing (5) attached to the testing machine.

Simulation analysis using FEMM 4.2 software was used to predict the magnetic distribution during MRE bushing testing. In this FEMM study, aluminum was preferred first in all material testing parts considering this aluminum is non-magnetic material. Besides that, 18 AWG-coated copper wire with a diameter of 1.02 mm has been selected to generate the magnetic field in the MRE bushing. A total

number of 1,000 coil turns were chosen together with the current application of 1 Amp in coil bobbin with 2 mm thickness. These FEMM conditions were used as a basic guideline to understand the magnetic distribution behaviour. Finally, at the end of the FEMM analysis, the material testing parts were compared between aluminum (non-magnetic material) and mild steel (magnetic material) to investigate their magnetic distribution analysis in MRE bushing testing.

3. Results & Discussion

3.1. Magnetic Distribution Factors

Figure 2 shows a 2D axisymmetric of testing parts; MRE bushing, coil bobbin, and testing jig used in MRE testing, and each part was defined and labeled with material parts. Principally, aluminum was selected as a control material for all parts. The magnetic flux density was observed and measured in the effective area (red dotted line) and the measured length (green dotted line) was located in the middle part of the effective area and also perpendicular to the magnetic flux direction. As the materials for each part have been defined, the FEMM software was started with meshing the nodes and simulating the magnetic circuit in the design (Figure 3). The highest magnetic flux density was aimed at the effective area where the MRE was placed.

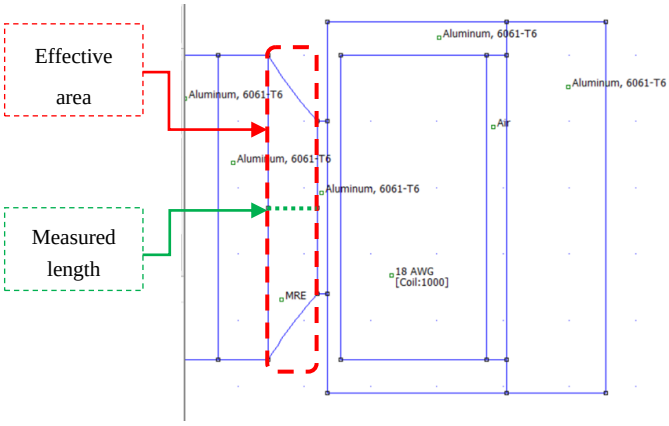

Figure 2. 2D axisymmetric diagram for testing parts for MRE testing; MRE bushing, coil bobbin, and testing jig.

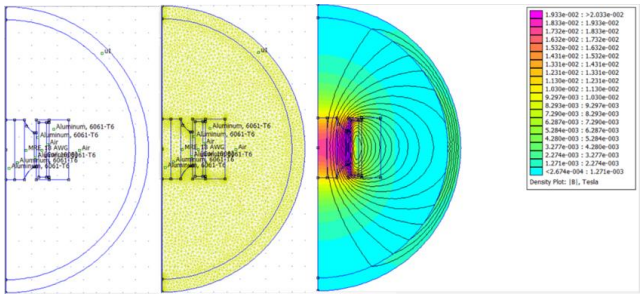

Figure 3. Design, meshing, and simulation results using FEMM software.

Magnetic distribution is affected by several factors. An investigation for each factor should be carried out to understand the behaviour of the magnetic distribution and also to know factors that can contribute to promising magnetic flux density during testing. Among the factors that can affect the magnetic distribution are coil bobbin thickness, coil diameter, number of coils turns and current (Amp) applied to the system. The magnetic flux density was observed in the effective area and measured along the measured length.

The effect of coil bobbin thickness on magnetic flux density, B (miliTesla: mT) is shown in Figure 4. The magnetic flux density becomes slightly higher when thinner coil bobbin thickness was used in the analysis. The magnetic flux density recorded for 2 mm and 4 mm of coil bobbin thickness was 16.9 mT and 16.3 mT, respectively. This result indicates that the coil bobbin thickness does not give a significant impact on the magnetic flux density value.

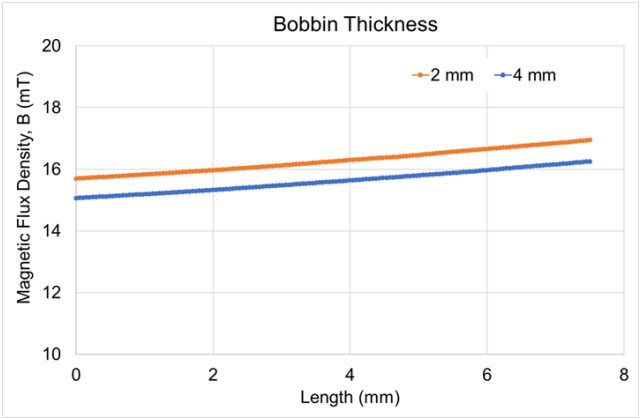

Figure 4. The magnetic flux density as a function of MRE measured length with different coil bobbin thicknesses.

The analysis with the magnetic flux density with different coil diameters (0.8, 1.0, 1.3, and 1.6 mm) is shown in Figure 5. The results depict that a larger coil diameter provides a higher magnetic flux density with the data recorded for 0.8 mm and 1.6 mm of coil diameter was 16.2 mT and 18.4 mT, respectively.

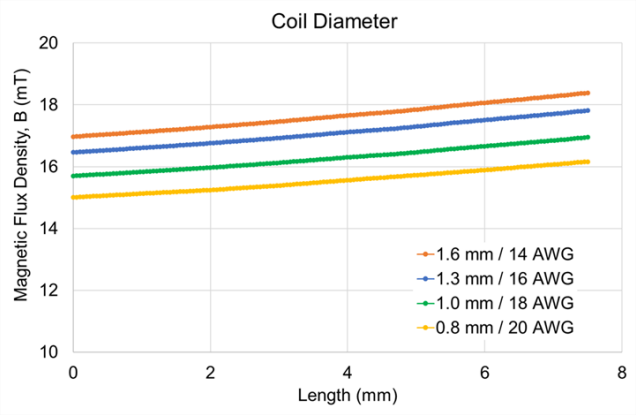

Figure 5. The magnetic flux density as a function of MRE measured length with different coil diameters.

Next, the influence of the number of coil turns on the magnetic flux density was investigated. Four (4) different number of coil turns were investigated; 500, 1000, 1500, and 2000 turns. The results in Figure 6 show that the magnetic flux density increased with the increasing number of coil turns. The highest magnetic flux density value was 27.7 mT with the usage of 2000 turns of coils.

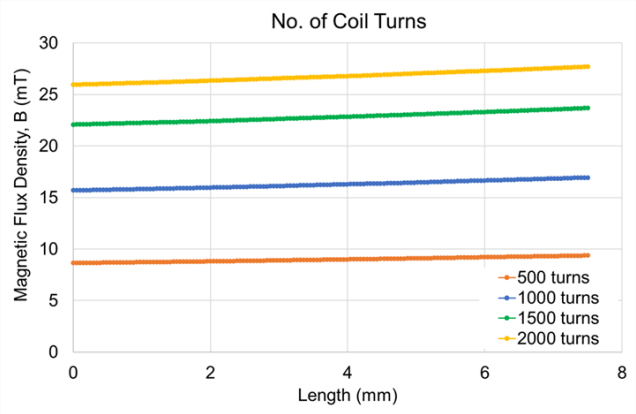

Figure 6. The magnetic flux density as a function of MRE measured length with different number of coils turns.

Finally, the implementation of different current (Amp) values applied to the MRE testing design was studied. The results of the magnetic flux density with different currents applied at 1, 10, and 20 Amp are shown in Figure 7. The data obtained show that the magnetic flux density increased dramatically with the increase of current applied. The magnetic flux density increased from 16.9 mT at 1 Ampere to 339 mT at 20 Ampere. This observation suggests that the current applied is the most prominent factor that affects the magnetic flux density value.

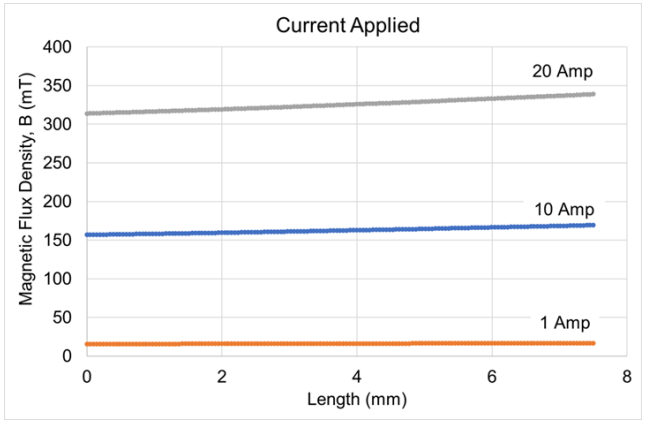

Figure 7. The magnetic flux density as a function of MRE measured length with different currents applied.

3.2. The B-H Relationship

The B-H curve relation represents the magnetic flux density, B, and the magnetic intensity, H (kA/m). These two magnetic characteristics are required for modelling in FEMM analysis. However, the relation curve for these two parameters is not fully understood for MRE. Therefore, Khanouki *et al.* [8] suggests to use B-H relation curve of magnetorheological fluid MRF for MRE modelling in FEMM analysis, with considering that MRE and MRF have similar mechanisms in responding to a magnetic field. The B-H relation curve of MRF was referred from the technical data of MRF with the commercial name MRF-132DG [13] issued by LORD Corporation.

As for the FEMM modelling purpose, curve fitting for the B-H relation curve was carried out to see the relationship between magnetic field intensity and magnetic flux density [8]. The relationship between these two magnetic characteristics can be expressed in the following form:

$$H_{MRE} = ((2.89 \times 10^2) \times B^2) + ((3.4 \times 10) \times (B) \qquad (1)$$

where H_{MRE} is magnetic field intensity for MRE. The data obtained from the results is shown in Table 2.

Table 2
The B-H relation curve data.

Magnetic Flux Density, B (mT)	Magnetic Field Intensity, H (kA/m)
0	0.00
200	18.36
400	59.84
600	124.44
800	212.16
1000	323.00

Next, FEMM analysis on testing parts selection between aluminum and mild steel was carried out with the input from the B-H curve data. The material selection for testing parts was decided based on the results obtained in Figure 8. The data shows that the usage of mild steel testing parts can provide higher magnetic flux density than aluminum testing parts with the highest magnetic flux density recorded were 960 mT and 100 mT, respectively.

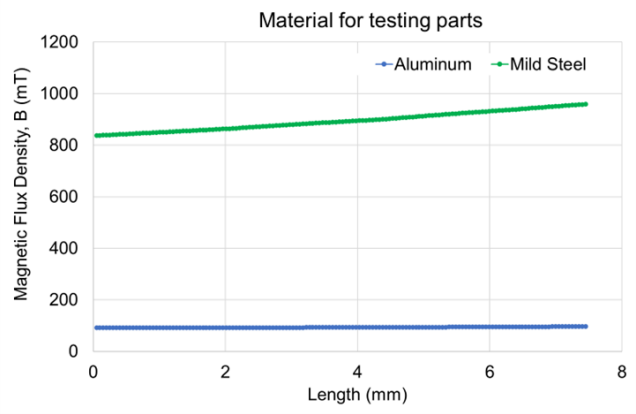

Figure 8. The magnetic flux density as a function of MRE measured length with different materials for testing parts.

The distribution of magnetic flux on the testing parts for aluminum and mild steel through FEMM analysis are shown in Figure 9. The usage of aluminum testing parts in Figure 9(a) have shown the magnetic flux distributed across beyond the testing structure. This observation suggests magnetic field leakage existed. In contrast, the mild steel testing parts in Figure 9(b) have shown the circulation of the magnetic flux throughout the entire testing structure. It can be seen that most of the magnetic flux was concentrated along the structure with no field leakage being observed, so that high magnetic flux density was generated in the MRE area or known as an effective area.

(a)

(b)

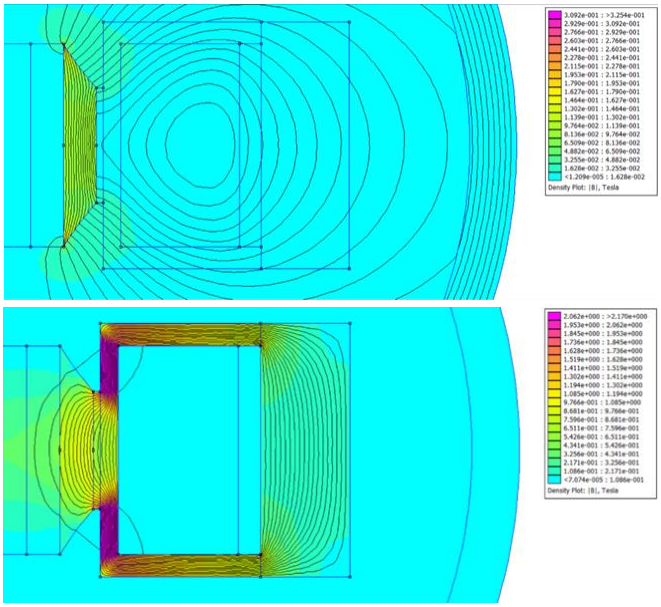

Figure 9. Magnetic flux distribution for testing parts (a) aluminum (non-magnetic material); (b) mild steel (magnetic material).

4. Conclusion

The application of FEMM software is becoming significant in MRE research recently. This software can predict the magnetic flux distribution during testing, and this will help MRE researchers to design the actual MRE testing so that the optimal magnetic flux density can be obtained at the MRE area. Electromagnets and permanent magnets are two approaches used in MRE research to supply the magnetic field during testing. In this study, an assembly of MRE testing using an electromagnet coil has been finalized by using a coil bobbin to wind the electromagnetic coil. This bobbin will be covered around the MRE bushing so that the magnetic field can be distributed throughout the MRE area. Analysis on the magnetic flux density for the MRE testing using FEMM 4.2 software was carried out with several factors that affecting this magnetic flux density such as coil bobbin thickness, coil diameter, number of coils turns and current (Ampere) applied to the test system. Among these factors, the current applied to the MRE testing provides the most significant factor that affects the magnetic flux density value. The magnetic flux density data recorded for 16.9 mT at 1 Amp and then increased drastically up to 339 mT at 20 Amp. Besides that, an implementation of the B-H relation curve data as input in modelling MRE testing has shown physical meaning in the FEMM analysis. The results on the material parts have shown that the usage of mild steel testing parts can provide higher magnetic flux density in the MRE effective area as compared to the aluminum testing parts. The highest magnetic flux density value was recorded for mild steel testing parts was 960 mT. Therefore, mild steel materials will be selected for the fabrication process for all testing parts in the real MRE bushing testing.

Acknowledgements

The authors would like to thank the Malaysian Rubber Board (MRB) for the research funding (Project ID: S21UKRP0756) and the permission to publish this paper. Assistance rendered by Mohd Affarizan Zainal Anuar and Nasrul Aiman Nazri is gratefully acknowledged.

REFERENCES

[1] H. X. Deng, X. L. Gong, and L. H. Wang, "Development of an adaptive tuned vibration absorber with magnetorheological elastomer.," *Smart Mater. Struct.*, vol. 15, pp. N111-6, 2006.

[2] B. Kavlicoglu, B. Wallis, H. Sahin, and Y. Liu, "Magnetorheological elastomer mount for shock and vibration isolation. Proceedings SPIE 7977 Active and Passive Smart Structures and Integrated Systems," 2011.

[3] I. Agirre-Olabide and M. J. Elejabarrieta, "A new magneto-dynamic compression technique for magnetorheological elastomers at high frequencies," *Polym. Test.*, vol. 66, no. January, pp. 114–121, 2018, doi: 10.1016/j.polymertesting.2018.01.011.

[4] Ubaidillah, S. Hadi, and Harjana, "Design and Fabrication of Magnetorheological Elastomer Vibration Isolator," vol. 5, no. 6, pp. 192–210, 2018.

[5] C. W. Lee, I. H. Kim, and H. J. Jung, "Fabrication and Characterization of Natural Rubber-Based Magnetorheological Elastomers at Large Strain for Base Isolators," *Shock Vib.*, vol. 2018, 2018, doi: 10.1155/2018/7434536.

[6] G. Priyandoko, P. Suwandono, N. R. Ismail, W. M. Utomo, and Ubaidillah, "Development of Vibration Isolator Magnetorheological Elastomer Based," *J. Phys. Conf. Ser.*, vol. 1908, no. 2021, 2021, doi: 10.1088/1742-6596/1908/1/012020.

[7] S. U. Khayam, M. Usman, M. A. Umer, and A. Rafique, "Development and characterization of a novel hybrid magnetorheological elastomer incorporating micro and nano size iron fillers," *Mater. Des.*, vol. 192, 2020, doi: 10.1016/j.matdes.2020.108748.

[8] M. Khanouki, R. Sedaghati, and M. Hemmatian, "Multidisciplinary Design Optimization of a Novel Sandwich Beam-Based Adaptive Tuned Vibration Absorber Featuring Magnetorheological Elastomer Mostafa," *Materials (Basel).*, vol. 13, no. 2261, pp. 1–22, 2020, doi: 10.1080/03052150701641866.

[9] M. A. Muhammad Fakhree *et al.*, "Simulation of a Pre-structure Device for Fountain-like Magnetorheological Elastomer via Finite Element Magnetic Method (FEMM)," vol. 12, no. 1, pp. 1–7, 2021.

[10] R. Mat Song *et al.*, "Semi-Active Controllable Stiffness Engine Mount Utilizing Natural Rubber-Based Magnetorheological Elastomers," *Front. Mater.*, vol. 9, no. April, pp. 1–12, 2022, doi: 10.3389/fmats.2022.875787.

[11] M. Ihsan, A. Hamid, S. A. Mazlan, and N. A. Nordin, "Design and Dynamic Stiffness Evaluation of Magnetorheological Elastomer Bushing using FEMM and Dynamic Testing Machine," vol. 20, no. 1, pp. 43–60, 2023.

[12] A. K. Bastola and M. Hossain, "A review on magneto-mechanical characterizations of magnetorheological elastomers," *Compos. Part B Eng.*, vol. 200, no. August, p. 108348, 2020, doi: 10.1016/j.compositesb.2020.108348.

[13] C. Lord, "Lord Technical Data: MRF-132DG Magneto-Rheological Fluid," *Lord Prod. Sel. Guid. lord Magnetorheol. fluids*, vol. 15, 2011, [Online]. Available: www.lord.com.